Accurate and Facile Determination of the Index of Refraction of Organic Thin Films Near the Carbon 1s Absorption Edge

Hongping Yan, Cheng Wang, Allison R. McCarn, and Harald Ade

Phys. Rev. Lett. **110**, 177401 — Published 23 April 2013

DOI: 10.1103/PhysRevLett.110.177401

Accurate and facile determination of the index of refraction of organic thin films near the carbon 1s absorption edge

Hongping Yan,[1] Cheng Wang,[2] Allison R. McCarn,[1,3] and Harald Ade[1]

[1] *Department of Physics, North Carolina State University, Raleigh, NC 27695, USA*
[2] *Advanced Light Source, Lawrence Berkeley National Lab, Berkeley, CA 94720, USA*
[3] *Present address: Department of Physics, University of Illinois at Urbana-Champaign, Urbana, IL 61801, USA*

(Dated: February 22, 2013)

A practical and accurate method to obtain the index of refraction, especially the decrement, δ, across the carbon 1s absorption edge is demonstrated. The combination of absorption spectra scaled to the Henke atomic scattering factor database, the use of Doubly Subtractive Kramers-Kronig relations, and high precision specular reflectivity measurements from thin films allowed the notoriously difficult to measure δ to be determined with high accuracy. No independent knowledge of the film thickness or density is required. High confidence interpolation between relatively sparse measurements of δ across an absorption edge has been achieved. Accurate optical constants determined by this method will greatly improve the simulation and interpretation of resonant soft X-ray scattering and reflectivity data. The method was demonstrated using poly(methyl methacrylate) and should be extendable to all organic materials.

The complex index of refraction describes the fundamental interaction, i.e. absorption and dispersion, of electromagnetic radiations with materials. These interactions in turn afford and support a plethora of materials characterization tools. Quite often, the quality of the analysis and optimization of experimental procedures or the exploitation of materials in applications ranging from devices to optical elements greatly benefit from an accurate knowledge of the complex index of refraction of the materials investigated. For this reason, optical constants of atoms and materials are catalogued and tabulated over the full range of the electromagnetic spectrum. In the energy range of $50 - 30,000$ eV, the optical constants have been compiled by Henke *et al.* in the form of atomic scattering factors $f(\omega) = f_1(\omega) - \boldsymbol{i} f_2(\omega)$ [1], which can be related to the scalar complex index of refraction, $\boldsymbol{n}(E) = 1 - \delta(E) + \boldsymbol{i}\beta(E)$ for disordered materials. A well-known limitation of the Henke data is the lack of fine spectral details to describe the optical properties near absorption edges. This is true for atoms, but even more so for compounds, for which the molecular bonding has to be taken into account. For organics, materials of primary concern here, the Near Edge X-ray Absorption Fine Structure (NEXAFS) has been compiled for numerous substances by a number of researchers as a supplement to Henke database [2–8]. Despite the remarkable richness of spectral features in these materials shown in NEXAFS spectra, corresponding databases and compilations for the dispersion properties are entirely lacking, other than a few reports on characterizing the dispersion of polyimide and amorphous carbon [9–11].

The recent development and utilization of Resonant Soft X-ray Reflectivity (R-SoXR) and Resonant Soft X-ray Scattering (R-SoXS) [12–15] has posed a greater need for precise knowledge about optical constants of related materials such as polymers. The strength of R-SoXR and R-SoXS is based on the strong elemental and chemical specific oscillations of the complex index of refraction of polymers near the absorption edge. Within the resonant region, both the relative dispersive *and* the absorptive properties of matter are important and can be selectively employed by simply tuning to the corresponding photon energies. Accurate knowledge of the complex index of refraction is a key aspect of utilizing R-SoXR and R-SoXS productively. Detailed knowledge of δ for a large range of materials will not only benefit R-SoXR and R-SoXS applications, but should be of wider interest including phase sensitive X-ray imaging methods [16].

In this letter, a facile yet accurate method to determine the index of refraction of a polymer material near the carbon 1s absorption edge is presented. This method takes advantage of the fact that NEXAFS of polymers can be relatively easily measured and, most importantly, that optical properties, i.e. δ and β, are directly fitted in model refinements of thin film reflectivity data. This allows the use of *Doubly* Subtractive Kramers-Kronig (DSKK) method to calculate δ from β accurately.

The absorption part of the index of refraction, β, can be easily measured in transmission geometry by applying Beer's Law, $I = I_0 \exp(-4\pi\beta z/\lambda)$, where I_0 is the incident intensity, I is the transmitted intensity through the film of a thickness z, and λ is the wavelength in vacuum. If z is accurately known, β can be obtained directly. The relative absorption can also be measured indirectly by using total electron yield measurements, although such a measurement is only semi-quantitative [5, 17–21]. In contrast, the dispersion part of the index of refraction, δ, is significantly more difficult to measure with high accuracy, especially for the fine structures near an absorption edge. Interferometry, ellipsometry, and reflectivity have been previously utilized to determine δ, and to a lesser extent β, for a limited number of materials [9, 10, 22–25]. For soft X-rays, the direct measurement of δ is complicated by the short wavelength (comparing to visible light), the small value of δ, and the relatively strong absorption. Although several types of interferometers have been developed to measure δ by measuring the phase shift of transmitted light through a thin film of the material of interest [9, 10, 22, 26], it is difficult to make interferometric measurements at, or close to, an absorption edge due to the high attenuation of soft X-rays [26]. These measurements also require an independent determination of the mass thickness of the film. An alternative way of measuring δ is by fitting the reflectance profile of a solid's surface to the Fresnel reflectivity to extract values for both δ and β. However, sample roughness and high absorption are known to affect the accuracy of these results [21]. Besides, the accuracy is also decreased for larger β/δ values.

The real and imaginary parts of the index of refraction are related through Kramers-Kronig (KK) relations within a semi-classical description of photon-material interaction [27] (see Supplemental Material for mathematical details). To avoid the relatively large error brought about by the substitution of infinite integration energy range with practically feasible finite range, we employ the subtractive method first introduced by Bachrach and Brown [28]. Specifically, we use *Doubly* Subtractive Kramers-Kronig (DSKK) method to calculate δ from β [29]:

$$\frac{\delta(E)}{(E^2 - E_a^2)(E^2 - E_b^2)} - \frac{\delta(E_a)}{(E^2 - E_a^2)(E_a^2 - E_b^2)} - \frac{\delta(E_b)}{(E_b^2 - E^2)(E_a^2 - E_b^2)} = -\frac{2}{\pi} P_C \int_{E_{Min}}^{E_{Max}} \frac{E'\beta(E')}{(E'^2 - E^2)(E'^2 - E_a^2)(E'^2 - E_b^2)} dE' \quad (1)$$

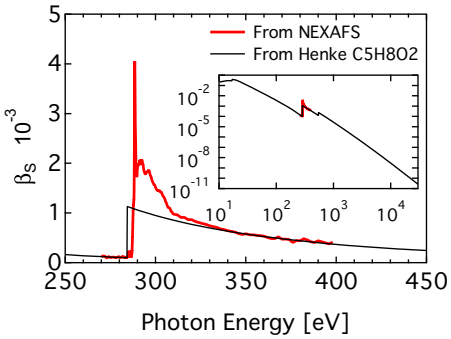

FIG. 1. Absorption spectra β (assumed density of 1 g/cm^3) calculated from transmission NEXAFS and Henke's atomic scattering factors. The inset shows the same plot with a broader energy range.

In this equation, the infinite integration interval is substituted by the finite range from E_{Min} to E_{Max}. The required two known δ values at E_a and E_b can be measured from reflectivity experiments as discussed later.

To further reduce the error caused by limited energy range, the NEXAFS absorption spectrum is expended using a "molecular scattering factor" constructed from Henke's atomic scattering factors to span the 10 eV to 30 KeV range of the integration variable. Although the readers are referred to the Supplemental Materials for detailed procedures, the overall method is described as follows:

1. $\beta_S(E)$ is calculated from NEXAFS that is extended with Henke's database. Here $\beta_S(E)$ is defined as $\beta(\rho, E)/(\rho/\rho_0)$, with $\rho_0 \equiv 1$ g/cm^{-3} and the density ρ a scale factor that needs to be determined to obtain β.

2. Using DSKK method with two required values $\delta(E_a)$ and $\delta(E_b)$ obtained from reflectivity experiments at below-edge and above-edge energies respectively, this preliminary β is utilized to predict the energy dependence of δ, which will then need to be scaled with the same scaling factor, ρ.

3. ρ is obtained by comparing reflectivity-measured δ at more energies (far away from absorption edge) to the predicted δ from last step.

4. ρ is then used to correct both the β and the predicted δ for energies in between E_a and E_b.

In this procedure, values of δ, instead of β, are used to determine the density. This is because δ is strongly energy dependent even when β is close to zero at below-edge energies (very little absorption), which allows accurate determination of the density in step 3 by comparing the reflectivity-measured to DSKK-predicted delta at both below-edge and above-edge energies, where the reflectivity measurements of δ and β are more precise.

The materials utilized to demonstrate the methodology is the ubiquitous polymer poly(methyl methacrylate) (PMMA), which is an amorphous polymer that does not show any anisotropy in the index of refraction and can be readily processed into a thin film. NEXAFS spectra of PMMA were acquired at beamline 5.3.2.2 at the Advanced Light Source (ALS) [30]. PMMA was spun-cast from n-butyl acetate with a thickness of $\sim$ 70 nm. The film was then floated off in deionized water and picked up with a TEM grid for NEXAFS spectra data acquisition. The absorption spectrum was measured from 270 eV to 400 eV in transmission. The samples for the reflectivity measurements were prepared from the same solution but on freshly cleaned silicon substrates. Reflectivity ($\theta - 2\theta$ geometry) data were acquired at ALS beamline 6.3.2 in a high vacuum [31], following previously established protocols [12] that includes precautions to avoid radiation damage which cause spectral changes [32]. Simulations and fits of reflectance were performed using the non-commercial program IMD [33] using a least-squared algorithm.

A molecular scattering factor $f_{2,C5H8O2}$ for PMMA (chemical formula $C_5H_8O_2$) is the sum of Henke's atomic scattering factors of 5 C, 8 H, and 2 O atoms. The calculated β_S from experimental NEXAFS spectrum and from $f_{2,C5H8O2}$ are plotted in Fig. 1. The NEXAFS data covers an energy range of 270 eV to 400 eV, while $f_{2,C5H8O2}$ ranges from 10 eV to 30 KeV. The step at $\sim$ 285 eV, also referred to as absorption edge, is due to the excitation of the core electron into the vacuum continuum. Since no molecular structure is considered in Henke's data, the edge looks like a step function with no details near the edge. The β_S calculated from $f_{2,C5H8O2}$ was then used to expand the NEXAFS spectra for energies lower than 270 eV and higher than 400 eV (see inset). The real part of the index of refraction, δ, then needs to be calculated using KK relations. To determine the density ρ mentioned above, R-SoXR was performed on a $\sim$ 70 nm PMMA film on silicon substrate. Reflectance measurements with θ from 0° to 20° were

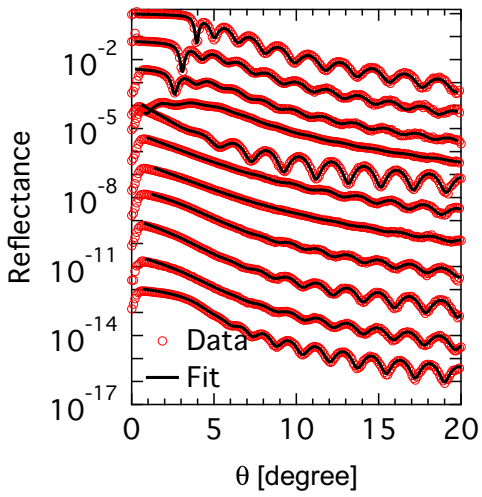

FIG. 2. Overplot of R-SoXR data (circle) and fits (line) for PMMA single layer, showing the quality of fits at energies, from top to bottom, 270, 282, 284, 286, 287.6, 288, 288.2, 288.6, 289, 294, and 310 eV.

performed for a set of energies spanning the $270 - 310$ eV range (Fig.2). Due to the strong energy dependence of the index of refraction, the resultant resonant aspects can be readily observed in the reflectance profiles. Below 285 eV, the reflectance profiles have strong Kiessig fringes at all angles. The onset of the first dip in the reflectance profile relates to the critical angle, θ_c, of the vacuum/PMMA interface, with $\theta_c \approx \sqrt{2\delta}$. For energies above the absorption edge, the reflectance profiles appear less modulated, especially at low grazing angles. This is due to the high absorption of the polymer at these energies and the long optical path the X-rays need to travel at small grazing angles. The reflected intensity corresponding to the polymer/substrate interface is reduced, leading to the small Kiessig fringe amplitudes at small angles. At higher angle, the optical path is shorter and less light is absorbed, which leads to better visibility of the interference fringes.

The experimental reflectance profiles are fitted through model refinements of a single layer by means of a least-square algorithm. It is most advantageous to start by fitting the reflectance data acquired at photon energies far below the absorption edge, e.g. 270 eV, where the sensitivity to δ is high. Parameters that describe the property of the film, such as the film thickness, roughness of the surface, and roughness at the polymer/substrate interface can be extracted with high accuracy. Since all data were obtained from the same sample, these structural parameters can then be used for fitting the reflectance profiles at all other energies. Therefore, only two variables, δ and β, are left as free parameters to be determined by a least-square fit.

With the values of δ obtained, the density of the PMMA thin film is determined by comparing the values derived from the reflectivity measurement (see Supplemental Material). From this linear fit, the density of the film is determined to be 1.20 ± 0.02 g/cm^3 (according to Equation 13 in Supplemental Material), which is very close to the tabulated value 1.18 g/cm^3 and falls into the literature values ranging from 1.17 to 1.22 g/cm^3. The value of the density is then subsequently used to calculate the accurate β with $\beta = (\rho/\rho_0)\beta_S$, followed by the application of DSKK method for the calculation of δ. β and δ are plotted in Fig. 3, along with the experimental results from fits of the reflectance measurements at key energies. Error bars in the experimental δ and β are reflecting the data scatter from fitting results obtained at multiple sample locations, which capture both the error of the fits themselves and the variations that come from the sample. Below the absorption edge, in the energy range of $270 - 287.6$ eV, the values of δ and β from the experiment and from the Kramers-Kronig calculations match well, and the experimental scatter for δ is small. For energies between 290 and 310 eV, systematic errors are observed. The present reflectivity fits slightly overestimate β and underestimated δ. This systematic error can be clearly seen by comparing the fits and data at the onset of the visibility of the Kiessig fringes in Fig. 2. The data shows the onset of fringes at smaller angles than the fit, indicating that the model fits overestimate the absorption in the actual films. For comparison, δ and β as derived from Henke's database are also shown in Fig. 3. We note that our method measures the film as prepared, which might contain impurities from supplier or a small amount of solvent despite the vacuum drying at elevated temperature [34, 35]. As the same film has been investigated by reflectivity and by transmission NEXAFS, it is really the agreement between these measurements (related via the KK transform) that is important. Careful inspection actually shows a small peak at around 285 eV that should not be there for pure PMMA. This peak is usually due to C=C π^* resonance according to Stöhr [17]. Considering the solvent used here (n-butyl acetate), this peak must due

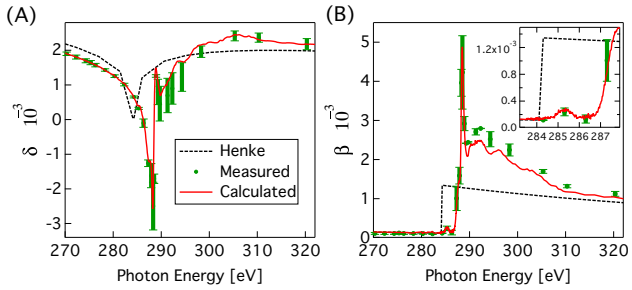

FIG. 3. Fitting results (dot) of optical constants, dispersion part δ (A), and absorption part β (B), for PMMA and calculation (solid line) using Kramers-Kronig relation. The corresponding values derived from Henke's database are shown for comparison (dashed line). The inset in (B) shows a zoom-in of the small absorption peak at around 285 eV due to impurities or additives.

to some other additives/contaminants rather than trapped solvent. In a testament to the R-SoXR measurements, that peak is also observed in the reflectivity data. The good agreement of experimental results and the calculation at large number of energy points especially the near-edge region shows the accuracy of the calculation and the validity of calculated value through the whole energy range. The optical constants of another sample polymer, polystyrene (PS), were also calculated and compared to experimentally derived values with good overall correspondence, indicating that the method is generally applicable. For details see Supplemental Material.

In conclusion, the indexes of refraction of a PMMA and a PS thin film were measured accurately for soft X-ray energies across the carbon 1s absorption edge using the inherent interferometric aspects of a reflectivity measurement from a thin film. Such a measurement is simpler and more straightforward to accomplish than a number of prior methods utilized to measure δ. The values of δ calculated with the DSKK method from measured β and a few calibrated δ's, and hence indirectly the accuracy of the NEXAFS spectrum, were verified at several energies by comparing with the experimental values of δ and β obtained from fitting the reflectance data using a least square fitting algorithm. The use of DSKK method is straightforward, yet decreases the error due to the limited energy range of β. By utilizing the presented method that combines NEXAFS measurements, Henke's atomic scattering factor database, reflectivity measurements, and Kramers-Kronig calculations, the index of refraction of polymer thin films can be determined with good accuracy in a self-consistent fashion without the need of independent mass thickness measurements. The dispersive properties of organic materials can now be tabulated in analogy to the databases already existing for β. With the necessity of access to a synchrotron facility acknowledged, the generality of this method should be applicable to a broad range of soft/hard materials.

The authors are grateful for the supplying of PMMA samples by C. R. McNeill (Monash University, Austrilia) and the fruitful discussions with B. Watts (PSI, Switzerland), E. M. Gullikson (ALS 6.3.2, CXRO) and A. L. D. Kilcoyne (ALS 5.3.2.2). Work at NCSU is supported by the U. S. Department of Energy (DE-FG02-98ER45737). Data acquired at beamlines 5.3.2.2 and 6.3.2 at the ALS, which is supported by the Director of the Office of Science, Department of Energy, under Contract No. DE-AC02-05CH11231.

[1] B. L. Henke, E. M. Gullikson, and J. C. Davis, Atom. Data Nucl. Data **54**, 181 (1993).
[2] O. Dhez, H. Ade, and S. Urquhart, J. Electron Spectrosc. **128**, 85 (2003).
[3] J. Kikuma and B. P. Tonner, J. Electron Spectrosc. **82**, 53 (1996).
[4] B. Watts *et al.*, J. Chem. Phys. **134**, 24702 (2011).
[5] S. Urquhart *et al.*, J. Electron Spectrosc. **100**, 119 (1999).
[6] S. Urquhart and H. Ade, J. Phys. Chem. B **106**, 8531 (2002).
[7] P. L. Cook *et al.*, J. Chem. Phys. **131**, 194701 (2009).
[8] K. Kaznacheyev *et al.*, J. Phys. Chem. A **106**, 3153 (2002).
[9] S. Dambach *et al.*, Phys. Rev. Lett. **80**, 5473 (1998).
[10] D. Joyeux, F. Polack, and D. Phalippou, Rev. Sci. Instrum. **70**, 2921 (1999).
[11] C. Jacobsen *et al.*, Proc. SPIE **5538**, 23 (2004).
[12] C. Wang, T. Araki, and H. Ade, Appl. Phys. Lett. **87**, 214109 (2005).
[13] S. Swaraj *et al.*, Nano Lett. **10**, 2863 (2010).
[14] H. Yan *et al.*, Adv. Funct. Mater. **20**, 4329 (2010).
[15] M. Mezger *et al.*, Phys. Rev. B **83**, 155406 (2011).
[16] M. Beckers *et al.*, Phys. Rev. Lett. **107**, 208101 (2011).
[17] J. Stöhr, *NEXAFS spectroscopy* (Springer, New York, 1992).
[18] H. Ade *et al.*, J. Electron Spectrosc. **84**, 53 (1997).
[19] E. M. Gullikson, P. Denham, S. Mrowka, and J. H. Underwood, Phys. Rev. B **49**, 16283 (1994).
[20] B. Sae-Lao and R. Soufli, Appl. Optics **41**, 7309 (2002).
[21] R. Soufli and E. M. Gullikson, Appl. Optics **37**, 1713 (1998).
[22] K. Rosfjord *et al.*, Appl. Optics **45**, 1730 (2006).
[23] H.-J. Hagemann, W. Gudat, and C. Kunz, J. Opt. Soc. Am. **65**, 742 (1975).
[24] J. Svatos *et al.*, Opt. Lett. **18**, 1367 (1993).
[25] R. Soufli and E. M. Gullikson, Appl. Optics **36**, 5499 (1997).
[26] C. Chang *et al.*, Opt. Lett. **27**, 1028 (2002).
[27] R. de. L. Kronig, J. Opt. Soc. Am. **12**, 547 (1926).
[28] R. Bachrach and F. Brown, Phys. Rev. B **1**, 818 (1970).
[29] K. F. Palmer, M. Z. Williams, and B. A. Budde, Appl. Optics **37**, 2660 (1998).
[30] A. L. D. Kilcoyne *et al.*, J. Synchrotron Radiat. **10**, 125 (2003).
[31] J. H. Underwood and E. M. Gullikson, J. Electron Spectrosc. **92**, 265 (1998).
[32] T. Coffey, S. Urquhart, and H. Ade, J. Electron Spectrosc. **122**, 65 (2002).
[33] D. L. Windt, Comput. Phys. **12**, 360 (1998).
[34] J. Perlich *et al.*, Macromolecules **42**, 337 (2009).
[35] X. Zhang *et al.*, Macromolecules **43**, 1117 (2010).